Macromolecular Materials and Engineering
www.mme-journal.de

Failure of Stretchable Organic Solar Cells under Monotonic and Cyclic Loading

*Oluwaseun Oyewole, Deborah Oyewole, Omolara Oyelade, Sharafadeen Adeniji, Richard Koech, Joseph Asare, Benjamin Agyei-Tuffour, and Winston Soboyejo**

Results of experimental and computational studies of failure of stretchable organic solar cells (SOSCs) are presented here. The SOSCs are produced by the deposition of poly(3,4-ethylenedioxythiophene):polystyrene sulfonate (PEDOT:PSS) anodic layers on prestretched poly(dimethyl-siloxane) (PDMS) substrates. This is followed by the deposition of active organic bulk heterojunction layers and cathodic eutectic gallium indium (EGaIn). Wrinkled structures are then formed by releasing the prestretched PDMS. The underlying failure associated with the formation of the wrinkled films is discussed, along with the subsequent mechanisms of deformation and cracking under monotonic and cyclic loading. Effects of monotonic and cyclic loading on the optical transmittance of the PEDOT:PSS layer and photoconversion efficiencies of the multilayered SOSC structures are also examined. An increase in the transmittance is observed as strain is applied to flatten the wrinkled structures. This enhances the power conversion efficiencies of the SOSCs as the strains increase from 0% to 32%. However, beyond this initial strain regime, the onset of overstretching decreases the optical transmittance and photoconversion efficiencies. The fatigue lifetimes of the layered SOSCs also decrease with increasing fatigue strain ranges between 10% and 25%. The decrease in the fatigue lifetimes is associated with a higher incidence of cracking and delamination.

In recent years, there has been an increasing interest in the applications of solar cells in electronics textiles[1–3] and roofing with corrugated architectures.[4] Since such applications require the stretching, bending, or twisting of layers within stretchable solar cells, there is a need to ensure that the layered constituents of the solar cells can be stretched,[1,2] twisted, or bent,[3,5] without inducing failure in their layers or interfaces. It is, therefore, of interest to study the effects of fatigue and failure on optoelectronic performance of stretchable organic solar cells (SOSCs).

Stretchable organic solar cells consist of multiple thin films that are deposited on stretchable substrates. Since some of the layers have limited "stretchability," it is important to disperse such materials in layers that increase the overall deformability of intrinsically elastic materials.[5,7] Solar cells can also be made more stretchable by wrinkling phenomena (that can be induced by the release of previously

Dr. O. K. Oyewole, R. K. Koech, Prof. W. O. Soboyejo
Department of Mechanical Engineering
Worcester Polytechnic Institute
100 Institute Road, Worcester, MA 01609, USA
E-mail: wsoboyejo@wpi.edu

Dr. O. K. Oyewole, D. O. Oyewole, Prof. W. O. Soboyejo
Materials Science and Engineering Program
Department of Mechanical Engineering
Worcester Polytechnic Institute
100 Institute Road, Worcester, MA 01609, USA

D. O. Oyewole
Physics Advanced Research Center
Sheda Science and Technology Complex
Abuja, Federal Capital Territory, Nigeria

O. V. Oyelade, S. A. Adeniji
Department Theoretical and Applied Physics
African University of Science and Technology
Km 10 Airport Road, Galadimawa, Abuja, Federal Capital Territory, Nigeria

The ORCID identification number(s) for the author(s) of this article can be found under https://doi.org/10.1002/mame.202000369.

DOI: 10.1002/mame.202000369

R. K. Koech
Department of Materials Science and Engineering
African University of Science and Technology
Km 10 Airport Road, Galadimawa, Abuja, Federal Capital Territory, Nigeria

Dr. J. Asare
Department of Physics
School of Physical and Mathematical Sciences
College of Basic and Applied Sciences
University of Ghana
Legon, Accra, Ghana

Dr. B. Agyei-Tuffour
Department of Materials Science and Engineering
School of Engineering Sciences
College of Basic and Applied Sciences
University of Ghana
Legon, Accra, Ghana

Prof. W. O. Soboyejo
Department of Biomedical Engineering
Worcester Polytechnic Institute
60 Prescott Street, Gateway Park Life Sciences and Bioengineering Center, Worcester, MA 01609, USA

stretched polymeric substrates) in films that are deposited after the stretching process.[1–9]

The early studies of the deformation of flexible thin-film metals on stretchable substrates were performed by Jones et al.,[10] Lacour et al.,[11–13] and Bowden et al.,[14,15] respectively. These studies focused largely on metallic thin films that were deposited on polymeric substrates. However, the onset of cracking in such structures occurred at relatively low strains. Furthermore, since most of these films were deposited using evaporation or e-beam techniques, significant residual stresses[13,16–18] were induced in the films due to the thermal expansion mismatch between the films and the substrates.

A number of authors have studied the deformation and cracking mechanisms in metallic thin films deposited on stretchable substrates.[11,13–15,17,18] These include studies by Lacour et al.,[13] who have studied the electrical properties of stretchable gold films. The failure mechanisms associated with the elastic–plastic deformation of nanoscale gold layers on poly(dimethyl-siloxane) (PDMS) substrates have also been reported in the literature.[17–19] These studies have shown that failure can occur by film buckling, cracking, and delamination.[17,19] Suo et al.,[20] Tucker et al.,[21] Jia et al.,[22] and Huang et al.[23] have proposed mechanics models for the prediction of failure mechanisms in stretchable electronic structures. It is important to note here that wrinkling corresponds to surface roughening without delamination, while buckling corresponds to surface roughening with delamination.[24,25]

In an effort to develop robust structures of solar cells that can deform by stretching and/or bending, significant efforts have been made to deposit inorganic and organic solar cells on stretchable or flexible substrates.[1–4] Lipomi et al.[1,2] have used buckling instabilities to increase the stretching characteristics of organic solar cells with power conversion efficiencies of ≈1.2%. These have been stretched to strains of about 27%. Rogers et al.[26] and Su et al.[7] have also studied the evolution of buckling and delamination in inorganic electronics subjected to repeated stretching and bending.

In the case of stretchable organic solar cells, interfacial failure can also occur between the adjacent layers in the solar cell structures.[27,28] This can also occur by buckling-induced delamination/interfacial cracking, which can cause the scattering of light that is meant for generation of excitons. Such scattering can disrupt transportation of charges that can cause degradation in the optoelectronic properties of stretchable electronic devices. There is, therefore, a need to develop a fundamental understanding of the adhesion/interfacial failure in layered structures of stretchable organic solar cells under fatigue. There is also a need to study the potential effects of cyclic loading on the optoelectronic properties of stretchable organic solar cells.

In prior efforts to understand the adhesion between layers that are relevant to organic solar cells, Yu et al.[29] and Tong et al.[27] have studied interfacial adhesion in stretchable and nonstretchable structures of organic solar cells and light-emitting devices. They have shown that the interfaces between layered mixtures of poly(3-hexylthiophene):phenyl-C61-butyric acid methyl ester (P3HT:PCBM) and poly(3,4-ethylenedioxythiophene):polystyrene sulfonate (PEDOT:PSS) exhibits the strongest adhesion, while the interface between the cathodic layer and photoactive P3HT:PCBM exhibits the weakest adhesion, among the interfaces that were examined in their work.[27,29] These studies assumed that adhesion occurred primarily as a result of interactions between bimaterial pairs.[27–32]

Nevertheless, the occurrence of prestretch-induced buckling and wrinkling has been shown to occur in stretchable organic solar cells; there have been only limited efforts[1–4,8,24] to study the effects of fatigue and failure on optical properties and photoconversion performance of stretchable solar cell structures. In this paper, a combined experimental and theoretical approach is used to study the fatigue behavior and failure of stretchable organic solar cells. First, computational models and simulations are used to obtain insights into the delamination and failure mechanisms in stretchable bimaterial pairs that are relevant to stretchable organic solar cells. The simulations are then validated with experiments before studying the effects of fatigue on optical properties and photoconversion efficiencies of layered stretchable solar cells. The implications of the current work are then discussed to improve the design of stretchable solar cells.

We conducted load controlled cyclic deformation tests on wrinkled layered structures of SOSCs to estimate fatigue lifetimes at different applied strains. The wrinkled structures were fabricated by depositing films onto prestretched fabricated PDMS substrates (see the "Experimental Section" for details). The prestretched PDMS substrates were then released to form wrinkled structures that are strectchable. The strain–number of cycles ($\varepsilon - -N$) of the layered films of stretchable solar cells are presented in **Figure 1**a. This shows plots of the total strain range as a function of the number of cycles for the polymeric PDMS substrate and the substrates coated with the layered films of stretchable solar cells. We find that the strain range of the PDMS substrate is ≈30% for over 4000 cycles at a maximum load of 7 N. For the thin-film-coated PDMS, the strain ranges were smaller initially over a certain number of cycles before increasing. This is because the coated PDMS substrates are stiffer than the bare PDMS substrates.

In the case of the coated PDMS structures that were cyclically deformed at a maximum load of 7 N, the strain ranges were ≈25% up to ≈200 cycles before increasing to the level of the bare PDMS substrates. The lifetimes, N_f, of the coated films were estimated as the numbers of cycles before the strain ranges begin to increase. Similar trends were observed for maximum loads of 2–4.5 N that resulted to total strain ranges of 10–15%. The lifetime of the stretchable thin film also increased with decreasing strain range (Figure 1a).

The above results are well characterized by the Coffin–Manson relationship $(\Delta\varepsilon/2 = \varepsilon_f^{'}(2N_f)^c)$,[33,34] where $\varepsilon_f^{'}$ and c are the fatigue ductility coefficient and exponent, while N_f and $\Delta\varepsilon_p/2$ are the number of cycles to failure and strain amplitude, respectively. More relationships between lifetime and stress/strain are provided in the Supporting Information for low- and high-cycle fatigue. By plotting the applied strain amplitude against the number of cycles to failure of the thin films (Figure 1b), the fatigue exponent of the bilayered structure (P3HT:PCBM/PEDOT:PSS) of the stretchable solar cells was estimated as − 0.3.

To explore the underlying failure mechanisms in the cyclically deformed wrinkled films, we carried out in situ observations of the film under an optical microscope, while further

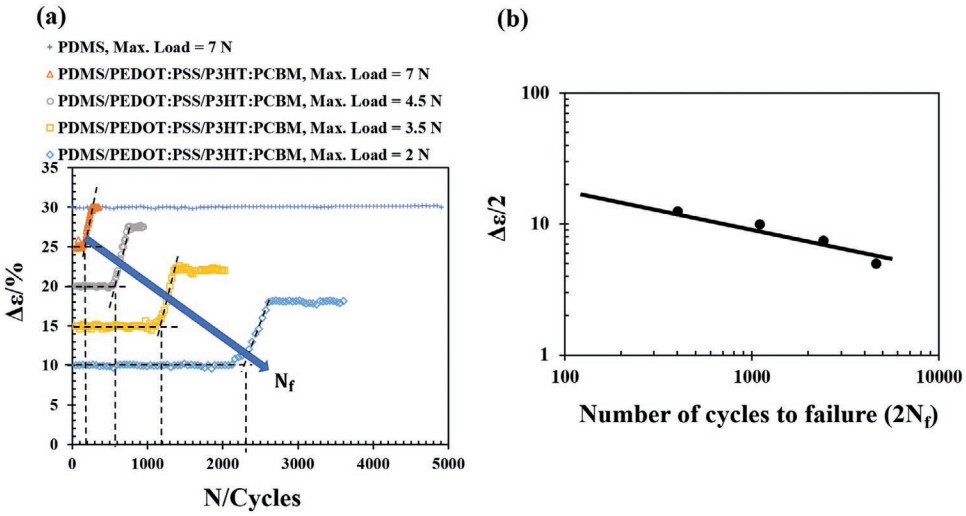

Figure 1. Fatigue behavior of layered stretchable solar cells. a) Strain range–number of cycles (ε–N) at different loads; downward arrow indicates the increase in the number of cycles to failure as the strain range decreases. b) Log–log plot of strain amplitude–number of cycles to failure.

observations were performed under scanning electron microscopy (SEM) for wrinkled films that were cycled to failure. The SEM images of the stretchable films that were cyclically deformed to failure at different strain ranges are presented in **Figure 2**. In the case of the unstretched sample of stretchable films (Figure 2a), the surface had a corrugated structure without any observable failures. The films are perfectly wrinkled without delamination (Figure 2a, inset). When the stretchable films were subjected to cyclic deformation at a strain range of 10%, cracks were along the crests of the corrugated films after

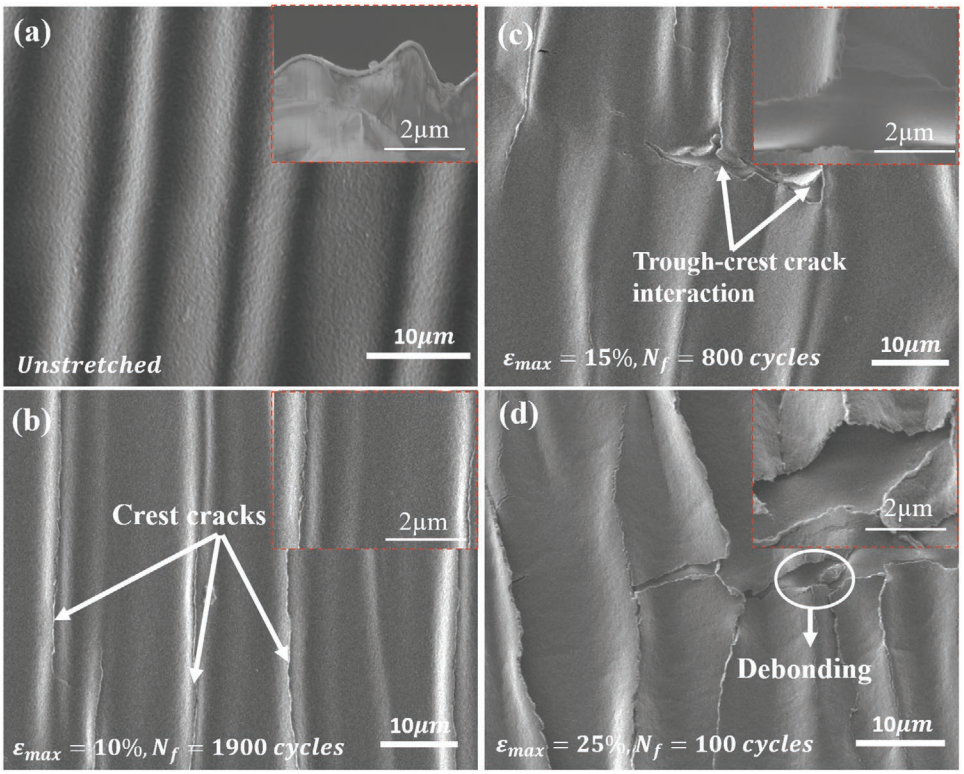

Figure 2. SEM images of fatigue failure modes of the stretchable P3HT:PCBM/PEDOT:PSS/PDMS substrate. a) Top surface of unstretched films with the cross section of the layered structure (inset). b) After 1900 cycles to failure with a maximum strain of 10% with evidence of fatigue cracks along the crest of the wavy structure. c) After 800 cycle to failure at 15% strain with evidence of crest–trough intercracking due to fatigue. d) After 100 cycles at 25%. The insets in panels (b)–(d) show higher-magnification images of cracking, delamination, and debonding of the cyclically deformed films.

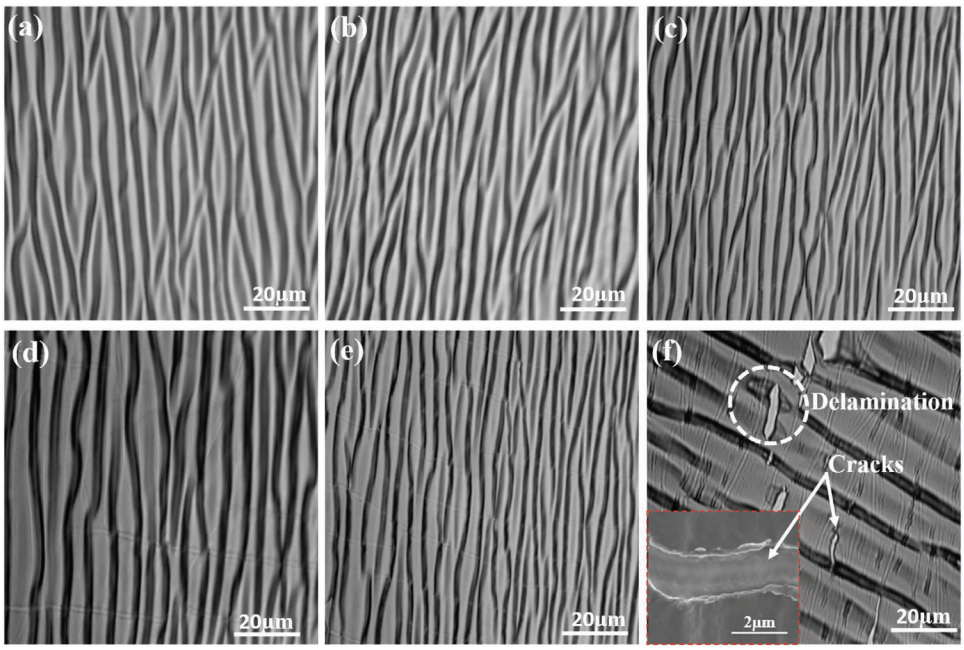

Figure 3. Optical microscopy images of stretchable P3HT:PCBM/PEDOT:PSS/PDMS substrate at different stages of cyclic loadings: a) 0 cycle, b) 20 cycles, c) 50 cycles, d) 100 cycles, e) 180 cycles, and f) 200 cycles showing a higher-magnification SEM image of cracks (inset). The strain range on this sample is 20%.

cycling for 1900 cycles (Figure 2b). For higher strain ranges between 10% and 25%, cracks were observed at the troughs and crests in the corrugations (Figure 2c) along with significant film delamination and debonding (Figure 2d). Higher-magnification images of the failure mechanisms in the stretchable films are also presented in Figure 2b–d (insets). In most cases, cracks initiate from the area of higher concentration of stresses, before trough–crest crack interactions in the corrugated films (Figure 2c). At a higher number of fatigue cycles, the films catastrophically debond from the substrates (Figure 2d).

The optical microscopy images of the cyclically deformed structures of the stretchable solar cells at 20% strain range are presented in **Figure 3**a–f, for different stages of fatigue failure. The results show clear evidence of cracks along and across the corrugations within the thin-film structures. However, the underlying PDMS substrate does not appear to be damaged by the cyclic deformation and cracking phenomena in the attached film structures as shown in the optical microscopy image (Figure 3f) and the higher magnification SEM image (Figure 3f, inset).

The performance of stretchable organic solar cells is dependent on the amount of light that the photoactive material can trap. This light travels through the transparent anodic PEDOT:PSS layer. It is, therefore, of interest to discuss the changes in the optical transmittance of these layers under monotonic deformation. We obtained the optical transmittance of the wrinkled films using Avantes UV–VIS–NIR spectrophotometer (Avantes BV, USA) under different monotonic strains. **Figure 4**a presents the measured optical transmittance of the stretchable anodic PEDOT:PSS layer at different strains. The optical transmittance initially increased with increasing monotonic strains between 0% and 32%, before a decrease in the transmittance at higher applied strains. The optical microscopy images (Figure 4b–d) correspond to the unstretched (Figure 4b), stretched (Figure 4c), and overstretched (Figure 4d) PEDOT:PSS.

The change in the transmittance (within the visible spectrum) of the stretchable PEDOT:PSS layers is attributed to the flattening of the wrinkled films and some observable failure mechanisms. When the film is moderately stretched (Figure 4c), the wavy structures undergo out-of-plane deformation. This increases their transmittance as the films are flattened.[35] However, the transmittance was found to decrease when the films are overstretched (Figure 4d). The reduction of the transmittance is associated with the transverse cracks that were observed in the films (Figure 4d). This suggests that the light that travels through such layers and interfaces can be scattered by the microcracks and possible interfacial cracks that are formed during the different stages of deformation. Since such cracks scatter light, the formation and growth of cracks can then reduce the intensity of light that is available for the generation of holes and electrons in the stretchable organic solar cells.

The deformation of stretchable solar cell was simulated using the ABAQUS software package (ABAQUS 6.16, Dassault Systèmes Inc., RI, USA). The detailed solutions of the interfacial energy release rates are presented in the Supporting Information along with the parameters used in the simulations. The stress distributions in the 3D structures, upon release of prestrained substrate, are presented in **Figure 5**a. The results show that stresses are concentrated along the crests and troughs of the wavy structure. These are consistent with the transverse and interfacial cracks that were observed in the experiments.

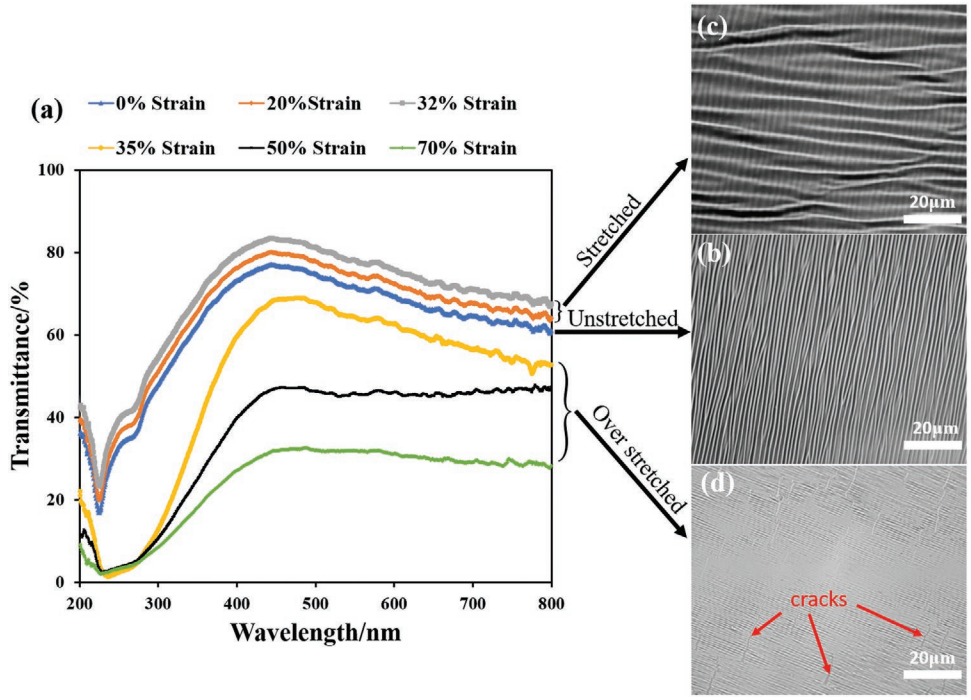

Figure 4. a) Effects of stretching on optical light transmittance of stretchable anodic PEDOT:PSS at different strain levels. b-d) Optical images of typical: unstretched b), stretched c), and overstretched d) samples of the stretchable PEDOT:PSS film.

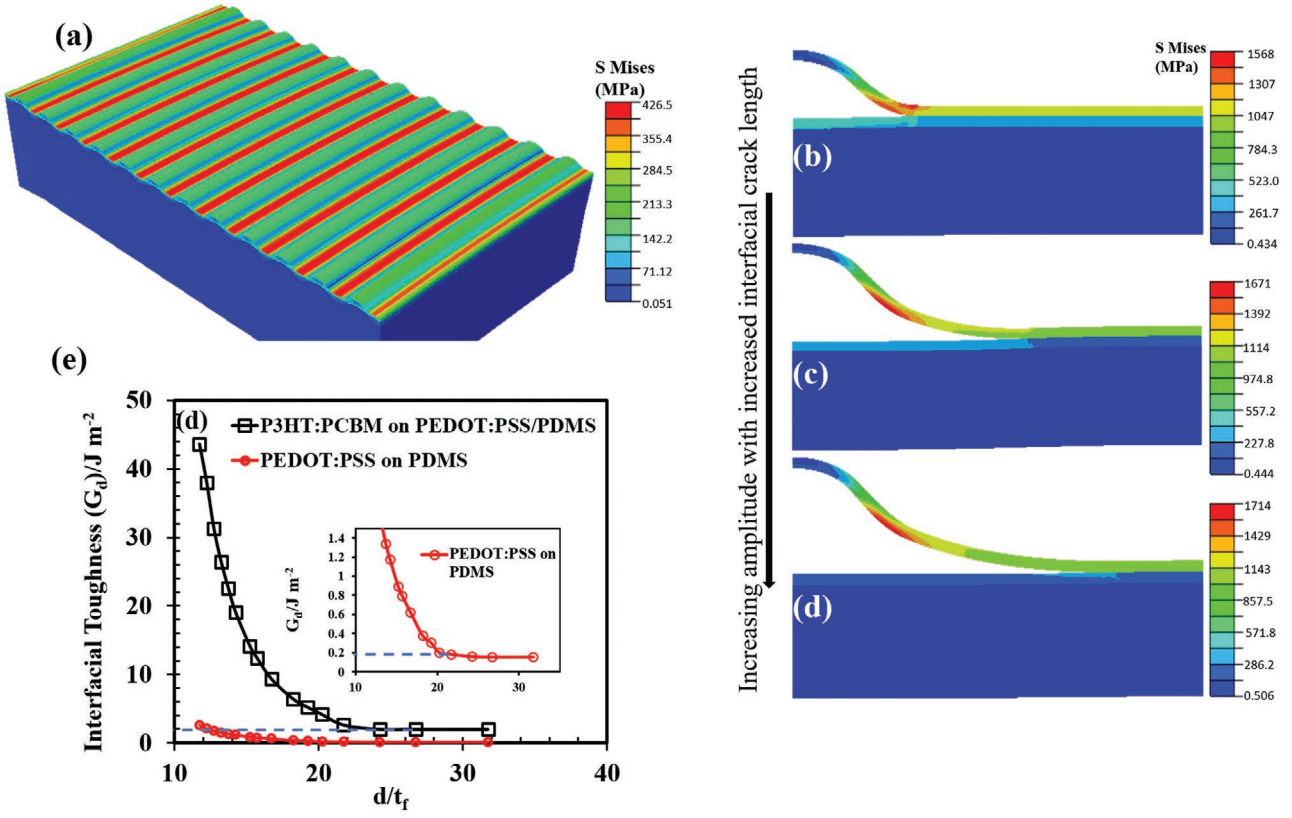

Figure 5. a) Von Mises of the stretched sample of stretchable P3HT:PCBM/PEDOT:PSS/PDMS, showing distribution of stresses. b–d) Von Mises of delamination-induced buckled P3HT:PCBM film on PEDOT:PSS/PDMS. The amplitude increases with increasing interfacial crack length. e) Interfacial toughness between the adjacent layers of stretchable solar cells as a function of the crack length. Interfacial toughness between PEDOT:PSS and PDMS (inset).

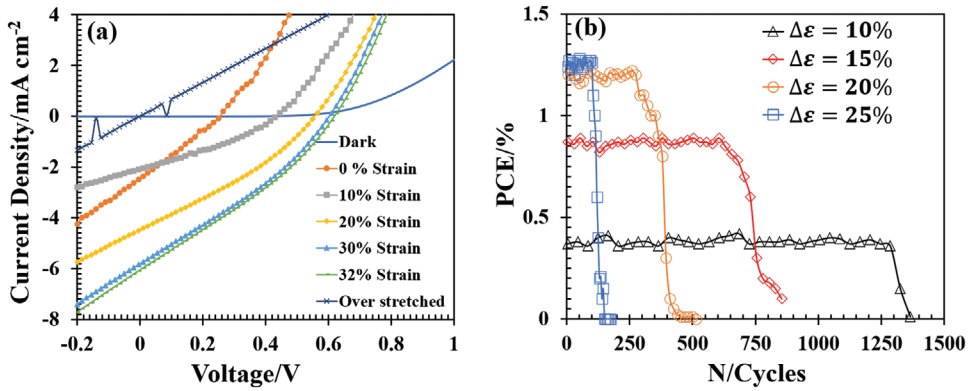

Figure 6. Effects of monotonic and cyclic loadings on electrical properties of stretchable solar cells. a) current density–voltage curves at different strains. b) Power conversion efficiencies of cyclically loaded stretchable solar cells at different strains.

For a scenario where delamination-induced buckling (Figure 2c,d) is evident during the deformation, the ABAQUS (ABAQUS 6.16, Dassault Systèmes Inc, Pawtuckett, RI, USA) software was used to calculate the critical interfacial toughness between adjacent layers of the stretchable structure. Figure 5b–d presents typical Von Mises stress distributions for the delamination-induced buckled P3HT:PCBM film on PEDOT:PSS/PDMS substrate.

The energy release rates at the tip of the interfacial crack are plotted against interfacial crack length (Figure 5e) for PEDOT:PSS/PDMS and P3HT:PCBM/PEDOT:PSS interfaces. The energy release rates decrease with the increasing crack length, but remain steady as the length of the crack extends into the steady-state regime. Similar results have been reported by Jia et al.[22] for layers of organic–inorganic multilayer permeation barriers in flexible electronic structures. The critical interfacial toughness values were obtained when the energy release rate reaches the steady-state condition.

The interfacial toughness between PEDOT:PSS and PDMS substrate is found to be ≈0.2 J m^{-2}, while the interfacial toughness between P3HT:PCBM and PEDOT:PSS is found to be ≈1.98 J m^{-2}. This value is close to the previously reported interfacial adhesion energies[28–30] and fracture toughness values[36] for the interface between P3HT:PCBM and PEDOT:PSS. The results show that the interface between P3HT:PCBM and PEDOT:PSS demonstrates higher interfacial toughness under deformation compared to the interface between PEDOT:PSS and PDMS. Hence, the evolving delamination of the stretchable solar cell structures (Figure 2b–d) can be initiated from the weak interface between PEDOT:PSS and PDMS.

Finally, we explored the effects of fatigue strain range on photoconversion of stretchable solar cells. The current density–voltage (J–V) curves obtained for unstretched and monotonically deformed stretchable organic solar cells are presented in **Figure 6**a. The areas under the J–V curves increase with increasing applied strain, for strains up to 32%. The short-circuit current density (J_{sc}) and the open-circuit voltage (V_{oc}) of the devices increased from 2.50 mA cm^{-2} and 0.25 V to 6.10 mA cm^{-2} and 0.61 V, when strained from 0% to ≈32%, respectively. The power conversion efficiency (PCE) also increased from ≈0.18% to ≈1.27% (Figure 6a). The increase in the device performance parameters (short-circuit currents, open-circuit voltages, and photoconversion efficiencies) is an indication that the active layer was able to absorb more light due to flattening of the wavy structures (as observed in Figure 4), leading to increased generation of holes and electrons. The increase in the device performance characteristics can also be attributed to an improved surface contact of the cathodic liquid metal (eutectic gallium indium (EGaIn)) due to flattening of the wavy structure as strains are applied to the SOSCs. A summary of the device parameters is presented in **Table 1**.

However, when the strain increases beyond the critical value, the PCEs of the devices decrease and J–V curves were straight lines when overstretched. This decrease in the PCEs is attributed to the effects of the transverse cracks and delamination that were observed (Figure 2b–d). Hence, limiting the applied strains to levels below the critical strains can maintain the mechanical integrity of the stretchable solar cells. The PCEs of the cyclically deformed stretchable solar cells are presented in Figure 6b for different applied strains. The results show that the lifetimes of the devices decrease, as the strain range increases.

In summary, we have used a combination of models and experiments to study the effects of monotonic and cyclic loading on the deformation and cracking behavior of thin films and multilayers that are relevant to SOSC structures. The changes in the current–voltage characteristics, optical transmittance, and photoconversion efficiencies of the organic solar cells are studied as a function of monotonic or cyclic

Table 1. In situ parameters of strained stretchable solar cells.

Applied strain [%]	J_{sc} [mA cm^{-2}]	V_{oc} [V]	FF	PCE (PCE$_{average}$) [%]
0	2.50	0.25	0.26	0.18 (0.15 ± 0.011)
10	2.04	0.43	0.33	0.32 (0.28 ± 0.021)
20	4.60	0.55	0.31	0.87 (0.76 ± 0.025)
30	6.00	0.56	0.32	1.20 (1.10 ± 0.024)
32	6.10	0.61	0.31	1.27 (1.1 ± 0.032)
70	0.00	0.00	0.00	0.00

loading. The observed deformation and cracking phenomena are consistent with the computed stress distributions and crack driving forces in the corrugated wrinkled structures. The fatigue lifetimes are also predicted using a Coffin–Manson expression. Failure of the SOSC structures is shown to be associated with the initiation of longitudinal/transverse cracks, as well as interfacial cracks between the PEDOT:PSS layers and the PDMS substrates.

The optoelectronic properties of the layered stretchable solar cells are also found to be influenced by the observed failure mechanisms that occurred under monotonic and cyclic loading. The transmission of light (through the stretchable anodic PEDOT:PSS layer) is found to increase with increasing applied strains up to 32%. The initial applied strains flatten the wavy structure and, thus, enable the passage of light to the active layer. This results in an increase in the transmittance, and it leads to the enhanced power conversion efficiencies of the SOSCs, for increasing strains between 0% and 32%. However, beyond this initial stretching regime, the overstretching of the SOSC structures results in transverse/longitudinal cracking and interfacial cracking that give rise to the delamination of the thin films (from the interfaces between the PEDOT:PSS layers and the PDMS substrates) in the SOSC structures. The fatigue lives of the flexible thin-film SOSC structures are also shown to be well characterized by the Coffin–Manson model, while the failure phenomena observed under monotonic and cyclic loading are shown to degrade the current–voltage characteristics and photoconversion efficiencies of the SOSCs, and the transmittance of the PEDOT:PSS anode.

Experimental Section

Processing of Layered Stretchable Organic Solar Cells: PDMS was fabricated by mixing a Sylgard 184 silicone elastomer base with a Sylgard 184 silicone elastomer curing agent in a 10:1 weight ratio. The mixture was degassed in a vacuum oven with a pressure of 25 kPa. This was done for 60 min to remove the trapped bubbles. The degassed PDMS was then poured into a clean mould (with a shining silicon wafer base) with a depth of 0.5 mm. The PDMS was subsequently cured at 65 °C for 2 h before cutting it into dimensions of 20 mm × 30 mm × 0.5 mm. The PDMS was then slowly prestretched and attached to a glass slide using the previous technique. This was done while ensuring that the cured surface (against the silicon wafer) was oriented with its face exposed to the atmosphere. The surface of the PDMS was then cleaned with sticky tape, before further cleaning with a UV/ozone cleaner (Novascan, Main Street Ames, IA, USA).

A mixture of PEDOT:PSS (PEDOT:PSS, H. C. Starck, Newton, MA, USA), dimethylsulfoxide (DMSO, MiliporeSigma, MO, USA), and Triton X-100 (Triton, MiliporeSigma, MO, USA) was prepared with a volume ratio of 94:5:1. The dimethylsulfoxide was added to segregate the weak PSS for strong inter-PEDOT bridging. This increased the conductivity of PEDOS:PSS on PDMS. Triton X-100 was also added to increase the wettability of the PEDOT:PSS on PDMS. The mixture was then filtered using a 0.45 µm mesh filter before spin-coating onto the prestretched PDMS at 1000 rpm for 50 s. It resulted in a uniform transparent film with a thickness of ≈100 nm. The spin-coated PEDOT:PSS film was then annealed in air at 100 °C for 10 min. It was then transferred into a nitrogen-filled glove box.

In the glove box, 30 mg mL^{-1} of P3HT:PCBM (1:1 wt%) solution was spin coated onto the PEDOT:PSS at 800 rpm for 30 s and 3000 rpm for 50 s to achieve a thin film of ≈120 nm thickness. The solution was prepared by mixing P3HT (Sigma–Aldrich, MO, USA; regioregular, average M_w: 20 000–45 000) and PCBM (Sigma–Aldrich, >99.5%) in anhydrous chlorobenzene. The spin-coated P3HT:PCBM layer was annealed at 120 °C for 10 min. The thickness was measured from a cross-sectional SEM image of the film. A drop of EGaIn) (Sigma–Aldrich, MO, USA) liquid metal was then deposited (through a syringe) onto the annealed P3HT:PCBM to form a solar cell of ≈0.15 cm^2 device area. The prestretched PDMS substrate was then released to form the wrinkled stretchable solar cell. The schematics of the above procedure are presented in Figure S1a,b (Supporting Information).

Fatigue Experiments: Cyclic fatigue tests were performed on the wrinkled films using Servohydrolic Instron machine (Instron 8872, Instron, Norwood, MA, USA) that was instrumented with a 50 N load cell using the previous technique for a bilayered structure.[34] First, the polymeric PDMS substrates were cyclically loaded between a minimum load of 0 N to a maximum load of 7 N to obtain a strain range of ≈30% in the uniaxial direction. The cyclic tensile tests were then performed on the structures of stretchable solar cells: PEDOT:PSS/PDMS, P3HT:PCBM/PEDOT:PSS/PDMS, and EGaIn/P3HT:PCBM/PEDOT:PSS/PDMS. These structures were cyclically loaded between a minimum load of 0 N and maximum loads of 2–7 N. Based on these loading conditions, the wrinkled structures were then strained with constant total strain ranges between 10% and 25%. The strain ranges, which were estimated from the displacement of the Instron crosshead, were observed to increase after failure of the films. A typical sinusoidal curve of the cyclic loading is presented in Figure S1c (Supporting Information).

Characterization: The optical transmittance of the anodic layer (PEDOT:PSS-coated PDMS) of the stretchable solar cells was measured in situ under monotonic loading with different applied strains. This was done using an Avantes UV–VIS–NIR spectrophotometer (Avantes BV, USA). The PEDOT:PSS-coated PDMS was mounted on a strain gauge. Air was then used as a control to ensure 100% transmittance, before placing the mounted sample between a light source and a light detector. The light was focused on the sample through a quartz optical fiber sensor (AVASPEC, Avantes, BV, USA). The transmittance was then measured at different strains (between 0% and 70%). The images of the PEDOT:PSS-coated PDMS were observed during in situ monotonic loading. This was done using an OMAX optical microscope (OMAX 40–3000 × 18MP, Gyeonggi-do, South Korea). The images of cyclically loaded stretchable structures were also observed under an optical microscope and a scanning electron microscope (JEOL JSM-700F, Hollingsworth & Vose, MA, USA).

The current density–voltage (*J–V*) curves of the stretchable solar cells were measured using a Keithley 2400 source meter unit (SMU) system (Keithley, Tektronix, Newark, NJ, USA) that was instrumented with the Kickstart software package (Keithley, Tektronix, Newark, NJ, USA). The devices were tested under an Oriel solar simulator (Oriel, Newport Corporation, Irvine, CA, USA) with an AM 1.5 G of 90 mA cm^{-2}. Voltage was sourced from –0.2 to 1.0 V to measure current density. This testing procedure was carried out for unstrained and cyclically deformed stretchable solar cells.

Supporting Information

Supporting Information is available from the Wiley Online Library or from the author.

Acknowledgements

The authors are grateful to the World Bank (Pan African Materials Institute supported by the World Bank African Centers of Excellence Program; Grant No: P126974) and the Worcester Polytechnic Institute for financial support. The authors also thank the Nelson Mandela Institution and African University of Science and Technology (AUST) for their financial support.

Conflict of Interest

The authors declare no conflict of interest.

Keywords

cyclic deformation, failure mechanisms, optical transmittance, photoconversion efficiencies, stretchable organic solar cells

Received: June 10, 2020
Revised: August 23, 2020
Published online: September 13, 2020

[1] D. J. Lipomi, J. A. Lee, M. Vosgueritchian, B. C. K. Tee, J. A. Bolander, Z. Bao, *Chem. Mater.* **2012**, *24*, 373.
[2] D. J. Lipomi, B. C.-K. Tee, M. Vosgueritchian, Z. Bao, *Adv. Mater.* **2011**, *23*, 1771.
[3] Y. Zhang, S. Xu, H. Fu, J. Lee, J. Su, K.-C. H, J. A. Rogers, Y. Yonggang, *Soft Matter* **2013**, *9*, 8062.
[4] G. Dennler, C. Lungenschmied, H. Neugebauer, N. S. Sariciftci, A. Labouret, *J. Mater. Res.* **2005**, *20*, 3224.
[5] J. Lee, M. Shi, J. Yoon, M. Li, Z. Liu, Y. Rogers, *Adv. Mater.* **2011**, *23*, 986.
[6] Y. Sun, J. A. Rogers, *Adv. Mater.* **2007**, *19*, 1897.
[7] Y. Su, Z. Liu, S. Kim, J. Wu, Y. Huang, J. A. Rogers, *Int. J. Solids Struct.* **2012**, *49*, 3416.
[8] T. Sekitani, Y. Noguchi, K. Hata, T. Fukushima, T. Aida, T. Someya, *Science* **2008**, *321*, 1468.
[9] T. Sekitani, H. Nakajima, H. Maeda, T. Fukushima, T. Aida, K. Hata, T. Someya, *Nat. Mater.* **2009**, *8*, 494.
[10] J. Jones, S. P. Lacour, S. Wagner, Z. Suo, *J. Vac. Sci. Technol., A* **2004**, *22*, 1723.
[11] S. P. Lacour, S. Wagner, Z. Huang, Z. Suo, *Appl. Phys. Lett.* **2003**, *82*, 2404.
[12] S. P. Lacour, J. Jones, Z. Suo, S. Wagner, *IEEE Electron Device Lett.* **2004**, *25*, 179.
[13] S. P. Lacour, S. Wagner, R. J. Narayan, T. Li, Z. Suo, *J. Appl. Phys.* **2006**, *100*, 014913.
[14] N. Bowden, W. T. S. Huck, K. E. Paul, G. M. Whitesides, *Appl. Phys. Lett.* **1999**, *75*, 2557.
[15] N. Bowden, S. Brittain, A. G. Evans, J. W. Hutchinson, G. M. Whitesides, *Nature* **1998**, *393*, 146.
[16] A. G. Evans, J. W. Hutchinson, *Acta Metall. Mater.* **1995**, *43*, 2507.
[17] S. Midturi, *ARPN J. Eng. Appl. Sci.* **2010**, *5*, 72.
[18] O. Akogwu, D. Kwabi, S. Midturi, M. Eleruja, B. Babatope, W. O. Soboyejo, *Mater. Sci. Eng., B* **2010**, *170*, 32.
[19] O. Akogwu, D. Kwabi, A. Munhutu, T. Tong, W. O. Soboyejo, *J. Appl. Phys.* **2010**, *108*, 123509.
[20] Z. Suo, J. H. Prévost, J. Liang, *J. Mech. Phys. Solids* **2003**, *51*, 2169.
[21] M. B. Tucker, D. R. Hines, T. Li, *J. Appl. Phys.* **2009**, *106*, 103504.
[22] Z. Jia, M. B. Tucker, T. Li, *Compos. Sci. Technol.* **2011**, *71*, 365.
[23] R. Huang, J. H. Prévost, Z. Y. Huang, Z. Suo, *Eng. Fract. Mech.* **2003**, *70*, 2513.
[24] O. K. Oyewole, D. Yu, J. Du, J. Asare, D. O. Oyewole, V. C. Anye, A. Fashina, M. G. Zebaze Kana, W. O. Soboyejo, *J. Appl. Phys.* **2015**, *117*, 235501.
[25] O. K. Oyewole, *Ph.D. Thesis*, African University of Science and Technology **2015**.
[26] J. A. Rogers, T. Someya, Y. Huang, *Science* **2010**, *327*, 1603.
[27] T. Tong, B. Babatope, S. Admassie, J. Meng, O. Akwogu, W. Akande, W. O. Soboyejo, *J. Appl. Phys.* **2009**, *106*, 083708.
[28] O. K. Oyewole, J. Asare, D. O. Oyewole, B. Agyei-Tuffour, V. C. Anye, M. G. Zebaze Kana, W. O. Soboyejo, *Adv. Mater. Res.* **2015**, *1132*, 89.
[29] D. Yu, O. K. Oyewole, D. Kwabi, T. Tong, V. C. Anye, J. Asare, E. Rwenyagila, A. Fashina, O. Akogwu, J. Du, W. O. Soboyejo, *J. Appl. Phys.* **2014**, *116*, 074506.
[30] O. K. Oyewole, D. Yu, J. Du, J. Asare, V. C. Anye, A. Fashina, M. G. Zebaze Kana, W. O. Soboyejo, *J. Appl. Phys.* **2015**, *118*, 075302.
[31] V. Brand, C. Bruner, R. H. Dauskardt, *Sol. Energy Mater. Sol. Cells* **2012**, *99*, 182.
[32] D. M. Huang, S. A. Mauger, S. Frieddrich, S. J. George, D. Bumitru-LaGrange, S. Yoon, A. J. Moule, *Adv. Funct. Mater.* **2011**, *21*, 1657.
[33] S. Suresh, *Fatigue of Materials*, Cambridge University Press, Cambridge, MA **1999**.
[34] O. Kraft, R. Schwaiger, *Mater. Sci. Eng., A* **2001**, *319–321*, 919.
[35] M. Shrestha, G.-K. Lau, *Opt. Lett.* **2016**, *41*, 4433.
[36] S. R. Dupont, M. Oliver, F. C. Krebs, R. H. Dauskardt, *Sol. Energy Mater. Sol. Cells* **2012**, *97*, 171.